IN2P3 Prospectives 2020

GT05 Physique de l'inflation et énergie noire

Cosmic Inflation IV: Bolometric Interferometry for CMB Polarization B-Mode Detection

Porteurs: J.-Ch. Hamilton , Steve Torchinsky

Dominic Beck,[a] Jacques Delabrouille,[a] Josquin Errard,[a] Ken Ganga,[a] Yannick Giraud-Héraud,[a] Laurent Grandsire,[a] Jean-Christophe Hamilton,[a] Jean Kaplan,[a] Sotiris Loucatos,[a] Thibaut Louis,[b] Stefanos Marnieros,[d] Ludovic Montier,[c] Baptiste Mot,[c] Louise Mousset,[a] Francesco Nitti,[a] Steve Torchinsky,[a] Guillaume Patanchon,[a] Michel Piat,[a] Guillaume Stankowiak,[a] Vincent Venin[a]

[a]APC
[b]LAL
[c]IRAP
[d]CSNSM

1 Introduction

The detection of B-mode polarization in the Cosmic Microwave Background (CMB) is the subject of a worldwide effort due to its importance as a confirmation of the Inflationary model of Cosmology. A clear detection of polarization B-modes in the CMB is evidence of primordial gravitational waves expected during the inflationary phase in the earliest moments of the Universe. The scientific motivation for CMB polarization measurements, be it from ground or space on small or large angular scales, is elaborated in greater detail in other sections of the IN2P3 2019 Prospective exercise (see Cosmic Inflation I, II, & III).

Polarization in the CMB is expected to be a small fraction of the CMB signal itself while the B-mode component of polarization will be several orders of magnitude smaller again. As a result, the measurement of B-mode polarization is a difficult exercise of extracting a signal buried deep within other signals (the CMB E-mode but also foreground contamination and lensing) and noise. This requires very careful instrument design and implementation, with sophisticated data analysis to separate unwanted contributions from the B-mode signal.

2 Bolometric Interferometry

Bolometric Interferometry is the marriage of techniques bringing together the great sensitivity and large bandwith of bolometers and the instrumental control and high fidelity imaging of aperture synthesis.

An imaging interferometer measures "visibilities" which are the complex (amplitude and phase) correlations between each antenna pair (baseline). In radio astronomy, we record the visibilities directly. A "correlator" digitizes the signals and multiplies pairs of signals to produce a stream of complex numbers, each of which corresponds to the cross correlation product of an antenna-pair. Channelization of the bandpass permits signal processing of individual, very narrow bands, and for each channel the signal is nearly monochromatic. In radio astronomy, large bandwidths are achieved by adding more digital electronics.

A bolometric interferometer takes advantage of the high sensitivity and large bandwidth of bolometers while also benefitting from the calibration technique possible with an imaging interferometer. The spatial sampling of the sky is generated by placing a cluster of back-to-back horns that behave effectively as electromagnetic nozzles. This horn cluster creates the $u - v$ sampling of the aperture plane equivalent to what is done by a distribution of antennas in a radio array. For the bolometric interferometer, instead of sampling the signals and computing the cross correlations between antenna pairs, the interference pattern is imaged.

A single image of the interference pattern has all the information convolved together resulting in observing the sky through a *synthesized beam*. The shape of this synthesized beam is given by the combination of all individual baselines (all pairs of horns). The bolometric interferometer end up being a synthesized imager observing the sky through its synthesized beam just the same way as a classical imager observes the sky through the beam formed by the telescope. For calibration and instrumental systematics studies it is however crucial to extract the individual visibilities. By blocking all horns except two, we measure the interference pattern of that baseline [see 2]. For example, using a 20×20 cluster of horns, there are 400 horns making $n(n-1)/2 = 79800$ baselines which are needed to be observed individually for self-calibration.

Performance of the bolometric interferometer improves as the number of baselines increases. A larger cluster of horns provides more baselines, but this in turn must be sampled by a larger array of detectors in the focal plane. As a result, the overall sensitivity of the bolometric interferometer is indirectly a function of the number of detectors in so much as the focal plane must be large enough to match the horn cluster.

3 Spectral Imaging

The bolometric interferometer has the unique capability to do spectral imaging. This is achieved because the profile of the synthesized beam depends on frequency. As a result, the sky maps can be deconvolved as a function of frequency using the information of the beam profile [6]. QUBIC has demonstrated this possibility by measuring the synthesized beam at different frequencies within the 130 GHz to 190 GHz band.

The beam mapping measurement campaign for QUBIC produced a series of maps for each TES pixel in the detector array. This is 244 maps for each frequency for a total of 1220 maps. Figure 1 shows example maps for one TES at three frequencies. The main lobe and secondary lobes are clearly visible and match well with theory.

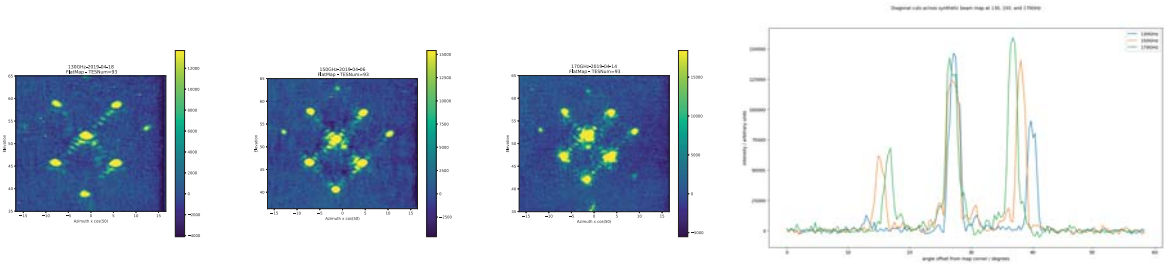

Figure 1. Maps of the synthetic beam for one TES at frequencies 130 GHz, 150 GHz, and 170 GHz. The plot on the right shows a diagonal cut of the synthetic beam with the coincident central lobe for each frequency and the secondary lobes which are closer to centre as frequency increases.

The secondary lobe locations depend on frequency while the main lobe is always at the same place (see right part of Figure 1). The secondary lobes are closer to centre as frequency increases, as expected. This is a key feature of the bolometric interferometer which makes spectroscopic imaging possible.

4 Map-making

Using the relative location and amplitude of all the peaks in the synthesized beam for each of the TES, we can now project the data onto the sky using optimal map-making to deconvolve from the effect of the multiple peaks. When observing the sky, this will result in an unbiased CMB map as has been showed using simulations. We have performed this with the calibration data in order to obtain an image of the point-like calibration source we have been using. The resulting image is shown in Fig. 2 exhibiting the expected point-source shape with a FWHM of 0.68 degree in excellent agreement with expectations.

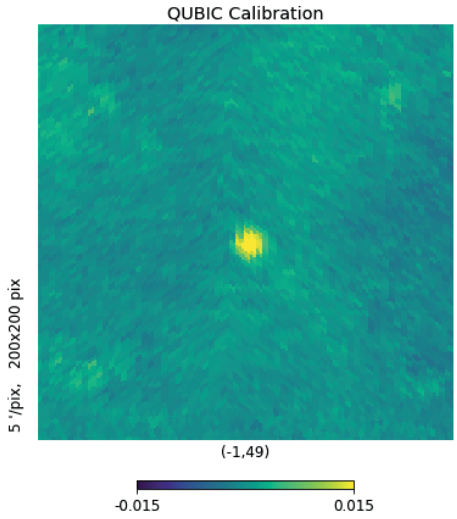

Figure 2. Calibration data with the source at 150 GHz projected on the sky using our map-making software to deconvolve from the multiple peaked synthesized beam. Small residuals of the deconvolved multiple peaks can be seen and are due to unmodeled non-linearity of the detectors due to saturation with the strong calibration source.

5 Self-Calibration

Self Calibration is a technique developed for aperture synthesis in radio interferometry. This technique evolved from the original idea in the 1970's of "phase-closure" [5, 7, 10] to become in the early 1980's "self-calibration" [4, 9]. See [3] for a detailed overview. Precise knowledge of the calibration source is not required, as long as it is a strong, point source. The large number of baseline visibilities allows us to solve for many unknowns, including the gain and phase corrections required, without having knowledge of the source.

In order to advance towards the full analysis of self-calibration, a key component is the ability to measure fringes. If fringes can be measured with a horn pair, then the full analysis can be done once the fringe measurement is done for all horn pairs. By measuring the fringe pattern of a single pair of horns we demonstrate the feasibility of doing self-calibration with the bolometric interferometer.

The QUBIC Technical Demonstrator successfully measured fringes between a pair of horns (Figure 3a). This is the derived image after comparing measurements of an image with all horns open, and an image with two horns closed. It is the equivalent of having all horns closed except the two [2]. The fringes are expected to be fainter in proportion to the distance to the centre of the focal plane (Figure 3b). This is not the case here because of saturation of the TES detectors. As a result, the fringe amplitude appears to be relatively constant, or near zero where saturated detectors were subtracted from one another. The problem with saturation was due to the cryogenic system which did not reach the optimum temperature for the TES. Future tests will work below the saturation point of the TES.

Figure 3. Left: Fringes measured on the QUBIC TES array. Fringes are clearly visible as bright, diagonal lines across the detector array. Right: Simulation of the fringe pattern expected to be measured with a baseline between horns 25 and 57. The fringe lines are in the same place as the measured image. The amplitude of the fringe lines are fainter with distance from the centre of the focal plane. This was not measured because of saturation of the detectors.

6 QUBIC: Q & U Bolometric Interferometer: Current and future

QUBIC is the first implementation of a bolometric interferometer. The current version is a Technical Demonstrator (QUBIC TD) operational in the laboratory of APC [1, 8]. This Technical Demonstrator is equipped with an 8×8 horn array and a focal plane equipped with 244 TES bolometers operating in the physical band 130-150 GHz. We plan to upgrade QUBIC to the Full Instrument (QUBIC FI) during 2020 with a 400 horns array and first 992 TES in the same band, then with 992 additional TES in the band 190-250 GHz when funding will have been obtained for the second band. Future possible upgrades include:

- Upgrade to multimoded optics by only changing the horns. This would lead to a factor ~ 5 sensitivity upgrade while improving spectro-imaging capabilities (larger secondary peaks in the synthesized beam due to top-hat shape of the multimoded horns beam).
- Multiple larger cryostats with more multimoded horns in each covering a larger bandwidth (from 90 to 300 GHz). For such a major upgrade we plan to use MKIDs instead of TES.
- Small scale Bolometric Interferometry can be achieved by installing an instrument similar to QUBIC (with slight optical modifications) at the focus of the neighbouring instrument in Argentina called LLAMA, a 12m antenna (clone of APEX) for which we have been asked to propose a possible instrument. This would open the path to all the sub-arcminute CMB polarization physics including lensing (neutrino masses, Dark Energy), Sunyaev-Zeldovith effect, ... (see "High Resolution CMB Physics" proposed by Th. Louis for these prospectives) but with the additional advantage of Spectro-Imaging offered by Bolometric Interferometry.

7 Conclusion

Bolometric interferometry is a technique developed at IN2P3 which has unique capabilities to eliminate instrument systematics through self-calibration, and improve foreground subtraction using spectral imaging. These capabilities are not found in classical imagers currently used for CMB B-mode experiments. Work on the Technical Demonstrator QUBIC has already shown the potential for this technique, putting IN2P3 in a position to play a significant role in the field CMB polarization studies and especially B-mode search.

Further development of the bolometric interferometry technique beyond the QUBIC Technical Demonstrator will lead to a powerful instrument, potentially with unrivaled purity of measurement. Such an instrument has the potential to achieve the very difficult measurement of the CMB B-mode polarization which is buried many orders of magnitude within an environment of noise and unwanted signals of terrestrial, galactic, and extra-galactic origin.

References

[1] Aumont, J. *et al.* [2016] *arXiv e-prints* , arXiv:1609.04372.

[2] Bigot-Sazy, M. A., Charlassier, R., Hamilton, J. C., Kaplan, J. & Zahariade, G. [2013] *A&A* **550**, A59, doi:10.1051/0004-6361/201220429.

[3] Cornwell, T. & Fomalont, E. B. [1999] "Self-Calibration," *Synthesis Imaging in Radio Astronomy II*, eds. Taylor, G. B., Carilli, C. L. & Perley, R. A., p. 187.

[4] Cornwell, T. J. & Wilkinson, P. N. [1981] *MNRAS* **196**, 1067, doi:10.1093/mnras/196.4.1067.

[5] Fort, D. N. & Yee, H. K. C. [1976] *A&A* **50**, 19.

[6] Hamilton, J.-C. *et al.*. [2020] *in preparation* .

[7] Högbom, J. A. [1974] *A&AS* **15**, 417.

[8] Mennella, A. *et al.* [2019] *Universe* **5**, 42, doi:10.3390/universe5020042.

[9] Pearson, T. J. & Readhead, A. C. S. [1984] *Ann. Rev. Astron. Astrophys.* **22**, 97, doi:10.1146/annurev.aa.22.090184.000525.

[10] Readhead, A. C. S. & Wilkinson, P. N. [1978] *ApJ* **223**, 25, doi:10.1086/156232.